Supporting Online Material for

Integrated sensing of multiple viral patterns by RIG-I via 5'-triphosphate dependent translocation on double stranded RNA

Sua Myong*, Sheng Cui, Peter V. Cornish, Axel Kirchhofer, Michaela U. Gack, Jae U. Jung, Karl-Peter Hopfner and Taekjip Ha

*To whom correspondence should be addressed. E-mail: smyong@uiuc.edu

This PDF file includes:

Materials and Methods

Protein purification

wtRIG and RIGh and the splice variant proteins were purified from Sf9 insect cells following the method previously published by Cui et al. (*1*)

RNA substrate preparation

For RNA used in Figures 1-2, (25bp dsRNA) the following RNA strands were purchased from Dharmacon. The sequence was adopted from HCV internal ribosome entry sequence.

5' (N6) GCU UGU CGG GAG CGC CAC CCU CUG C (3'-biotin) 3'
5' GCA GAG GGU GGC GCU CCC GAC AAG C (DY547-3') 3'

For the substrates used in Figure 3-4 DNA was purchased from IDTDNA.

5' - /5Biotin/ATA CAA ACA TTT TTA TTT CC/3Cy3Sp/ - 3'

5'- /5Biotin/ATA CAA ACA TTT TTA TTT CCT TTT TAA TTT /3Cy3Sp/ -3'

5'- /5Biotin/ATA CAA ACA TTT TTA TTT CCT TTT TAA TTT AAT TTA ATT A/3Cy3Sp/ -3'

5'- /5Biotin/ATA CAA ACA TTT TTA TTT CCT TTT TAA TTT AAT TTA ATT AAC AGT TGG TG/3Cy3Sp/ -3'

86mer ssRNA with 5'-triphosphate was in vitro transcribed;

The 86mer DNA template was cloned into pUC19 with a 3' HDV ribozyme to produce clean 3' ends. (*2*) The resultant plasmid was linearized with EcoRV (Invitrogen) and *in vitro* transcribed with purified T7 RNA polymerase using standard protocols. (*3*) The 86mer RNA was purified by denaturing PAGE and removed from the gel by the crush and soak method, which was followed by desalting using a NAP-10 column (GE Healthcare).

5'pppGGUUUUUCUU CUGAAGAUAA AGGUAAAGUG UCAUAGCACC AACUGUUAAUUAAAUUAAAU UAAAAAGGAA AUAAAAAUGU UUGUAU

Partial duplexes were prepared by mixing top and bottom strand oligos at a molar ratio of 1:1.6 (biotinylated : non-biotinylated strand) in 10mM Tris-HCl pH 8, 50mM NaCl and incubating at 80^{o}C for 2 minutes then slowly cooling to room temperature for 2 hour.

For RNA used in Figure S10, 25, 40 and 50 nts RNA was in vitro transcribed and biotinylated at 3' end and the sequence of transcript is as follows.

25mer ssRNA

5'ppp GCUUGUCGGGAGCGCCACCCUCUGC

35mer ssRNA

5'ppp GGAUCGAUCUGCUUGUCGGGAGCGCCACCCUCUGC

50mer ssRNA

5'pppGGCAGCUUCGACGUCAUAUCGAUCUGCUUGUCGGGAGCGCC ACCCUCUGC

3' biotinylation of RNA

Approximately 6 nmoles of RNA were oxidized by addition of sodium periodate (Sigma) to a final concentration of 20 mM. The reaction was quenched after 15 minutes and the RNA was subsequently labeled with biotin hydrazide (Sigma) by mixing overnight at 4C. Unincorporated biotin hydrazide was removed by multiple rounds of ethanol precipitation and phenol/chloroform extraction, which was followed by a final buffer exchange with a NAP-10 column (GE Healthcare).

Reaction condition for single molecule fluorescence assay

Prepared RNA substrate is immobilized on a quartz surface (Finkenbeiner), which is coated with polyethyleneglycol in order to eliminate nonspecificsurface adsorption of proteins(*4*). The immobilization was mediated by biotin-Neutravidin binding between biotinylated RNA of DNA, Neutravidin (Pierce), and biotinylated polymer (PEG-MW5,000, Nektar Therapeutics). About 100 pM of RNA molecules are immobilized. RNA density was checked via green laser. Then 100nM of wtRIG or RIGh protein was added with ATP (1uM-2mM) in buffer containing 20 mM Tris–HCl, pH 7.5, 5 mM MgCl2, 10 mM KCl, 4% (w/v) glycerol,in the presence of oxygen scavenging system of 1 mg/ml glucose oxidase (Sigma), 0.4% (w/v)D-glucose (Sigma), 0.04mg/ml catalase (Roche), and 1% v/v 2-mercaptoethanol (Acros). Measurements were taken at either room temperature for 5'-triphosphate RNA substrates or at 37^{o}C for dsRNA.

Single molecule fluorescence data acquisition and analysis

The programs used to analyze single molecule data are described in our previous work. (*5*) Emissions were collected from both donor (Cy3) and acceptor (Cy5) channels for consistency.

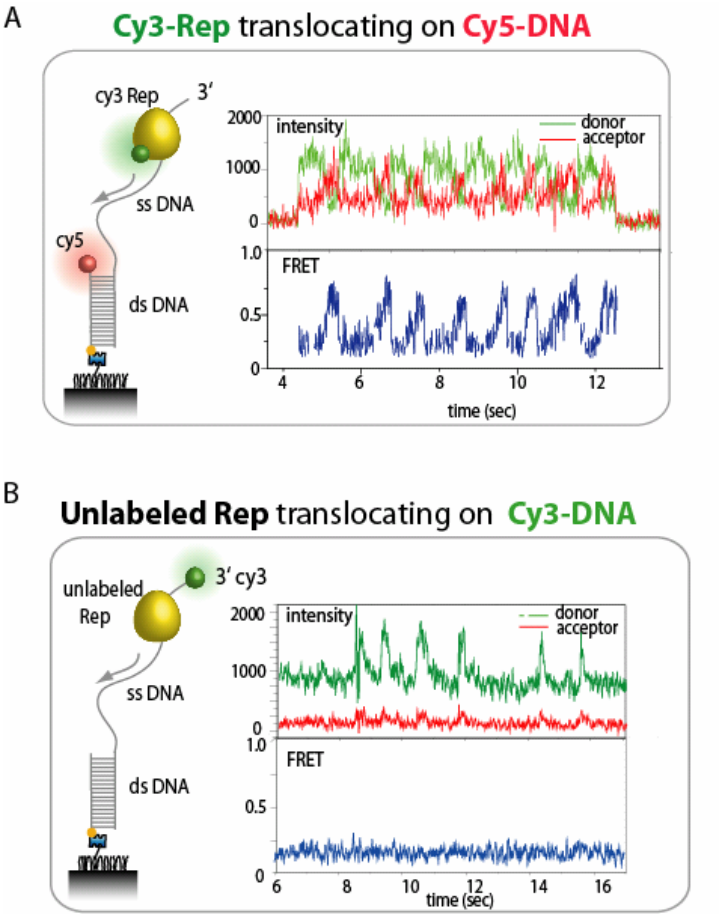

Fig. S1: Rep translocation can be visualized by single dye fluorescence change. A. Rep translocation on ssDNA was monitored by FRET. Rep was singly labeled with Cy3 and DNA was labeled with Cy5 at the junction of ssDNA and dsDNA. The experiment was performed at 22^{o}C with the following buffer composition: 10mM Tris-HCl, pH 7.6, 1mM ATP, 12mM MgCl2, 15mM NaCl, 10% glycerol (v/v), 200-400pM cy3-Rep and an oxygen scavenger system to slow photobleaching**.** The repetitive translocation of Rep on ssDNA in 3' to 5' direction was visualized by cycles of gradual FRET increase followed by abrupt FRET decrease. We have shown that Rep, as a monomer (200-400 pM) shuttles repetitively on ssDNA without unwinding duplex (*6*). B. The same activity was monitored on otherwise identical DNA substrate with single fluorophore (Cy3) at 3' end with unlabeled Rep.(lower panel) The pattern of intensity change i.e abrupt increase followed by a gradual decrease corresponds to Rep translocation from 3' to 5' direction, which is consistent with the FRET result obtained in the upper panel. The intensity change is due to enhanced fluorescence quantum yield caused by proximity of the protein. This validates the use of single fluorophore in monitoring protein motion.

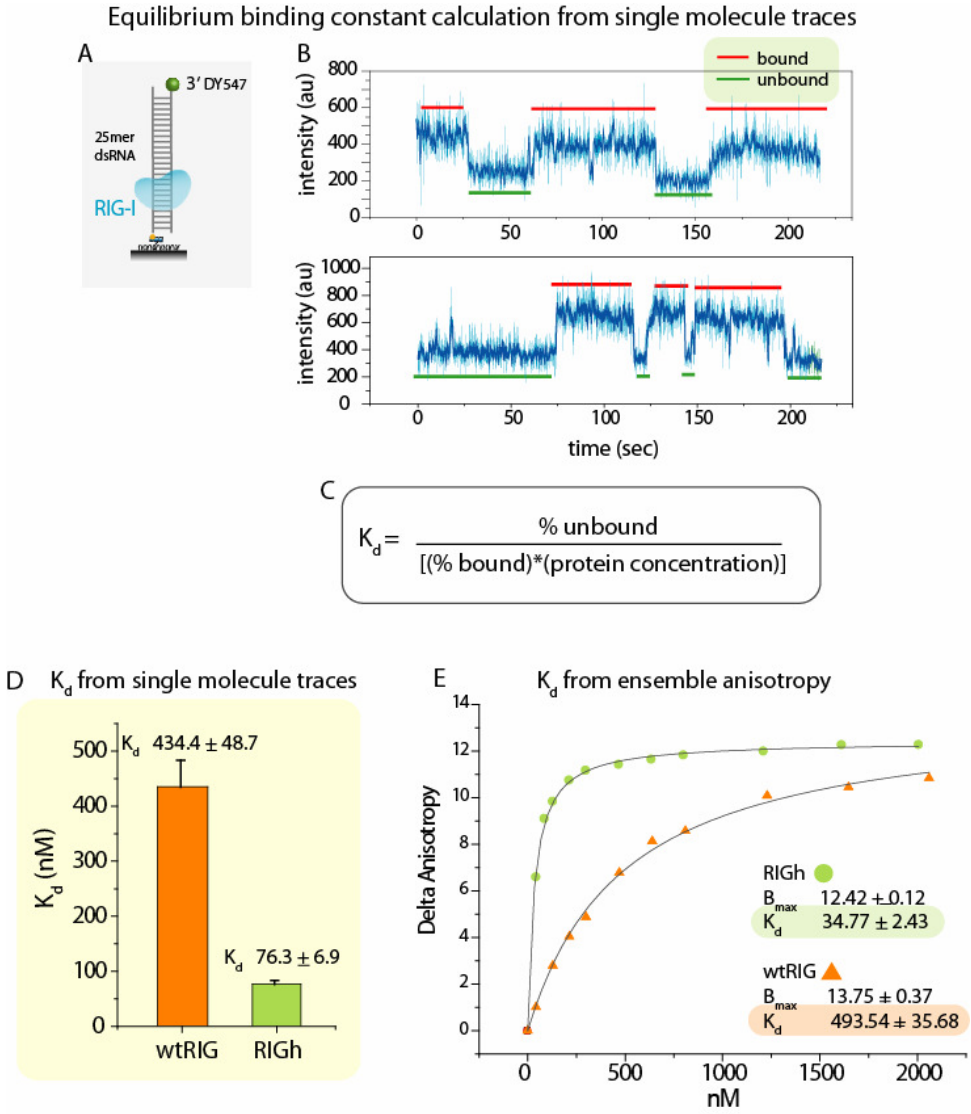

Fig. S2 : Equilibrium binding constant estimation from single molecule and ensemble measurement A, B The equilibrium binding constants for wtRIG and RIGh to dsRNA were calculated by using single molecule traces in the following way. 1. Single molecule traces were taken individually (200-300 molecules for each data set) 2. Protein-bound vs. unbound times were measured for each trace (B) 3. K_d was calculated by; **[% fraction unbound]/ [(% fraction bound)*(protein concentration)]** (C) 4. For wtRIG data taken at 100-300nM protein concentrations were used. For RIGh, data taken at 50-100nM protein concentrations were used. D. Calculation yields K_d (wtRIG) = 434 ± 49 nM; K_d (RIGh) = 76 ± 7 nM. E. The same substrate was used to measure K_d of wtRIG and RIGh using ensemble anisotropy and yields K_d (wtRIG) = 494 ± 36 nM; K_d (RIGh) = 35 ± 2 nM. K_d obtained from single molecule traces are within a factor of two of those obtained from the ensemble anisotropy measurement.

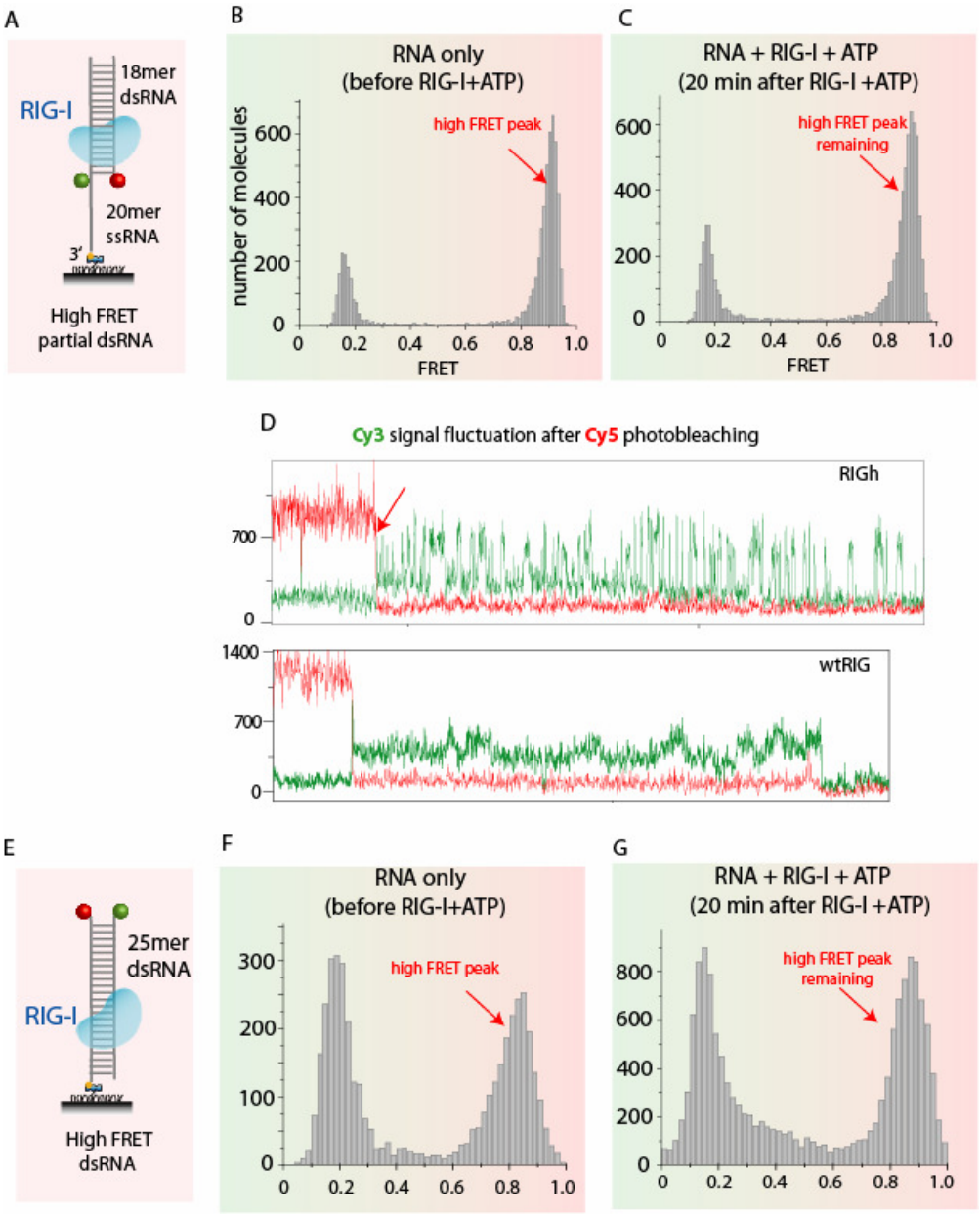

Fig. S3 : RIG-I does not unwind dsRNA A, E Two substrates were tested for RIG-I unwinding activity, 3' tailed partially duplexed RNA (A) and 25bp dsRNA (E) with FRET pair of dyes adjacent to each other so that unwinding can be detected by FRET decrease. Unwinding was performed by adding 100nM wtRIG or RIGh along with 1mM ATP at 37°C. B,C, F, G FRET histograms generated before and after the unwinding indicate that high FRET molecules remain high FRET without shifting to low FRET. D. Majority of traces show steady high FRET followed by acceptor photobleaching. A few traces show PIFE indicative of RIG-I translocation along dsRNA for both RIGh and wtRIG.

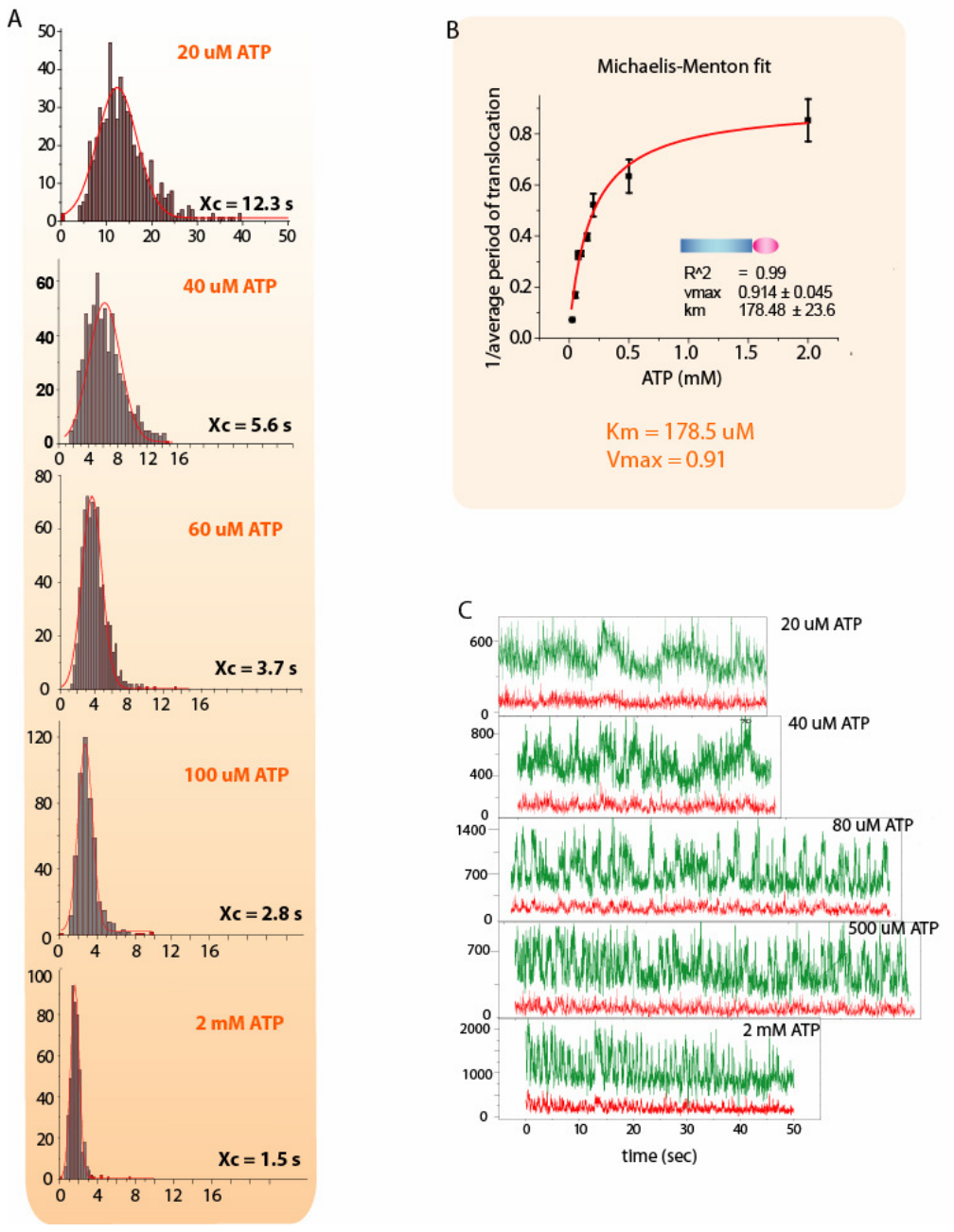

Fig. S4 : RIGh translocation on dsRNA is [ATP]dependent. A. Dwell time histograms for variable [ATP] clearly indicate that RIGh translocation on dsRNA is fueled by ATP hydrolysis. B. Michaelis-Menten fit gives K_m of 178.5uM and V_{max} of 0.914. C. Real time traces of single molecules taken at variable [ATP] conditions.

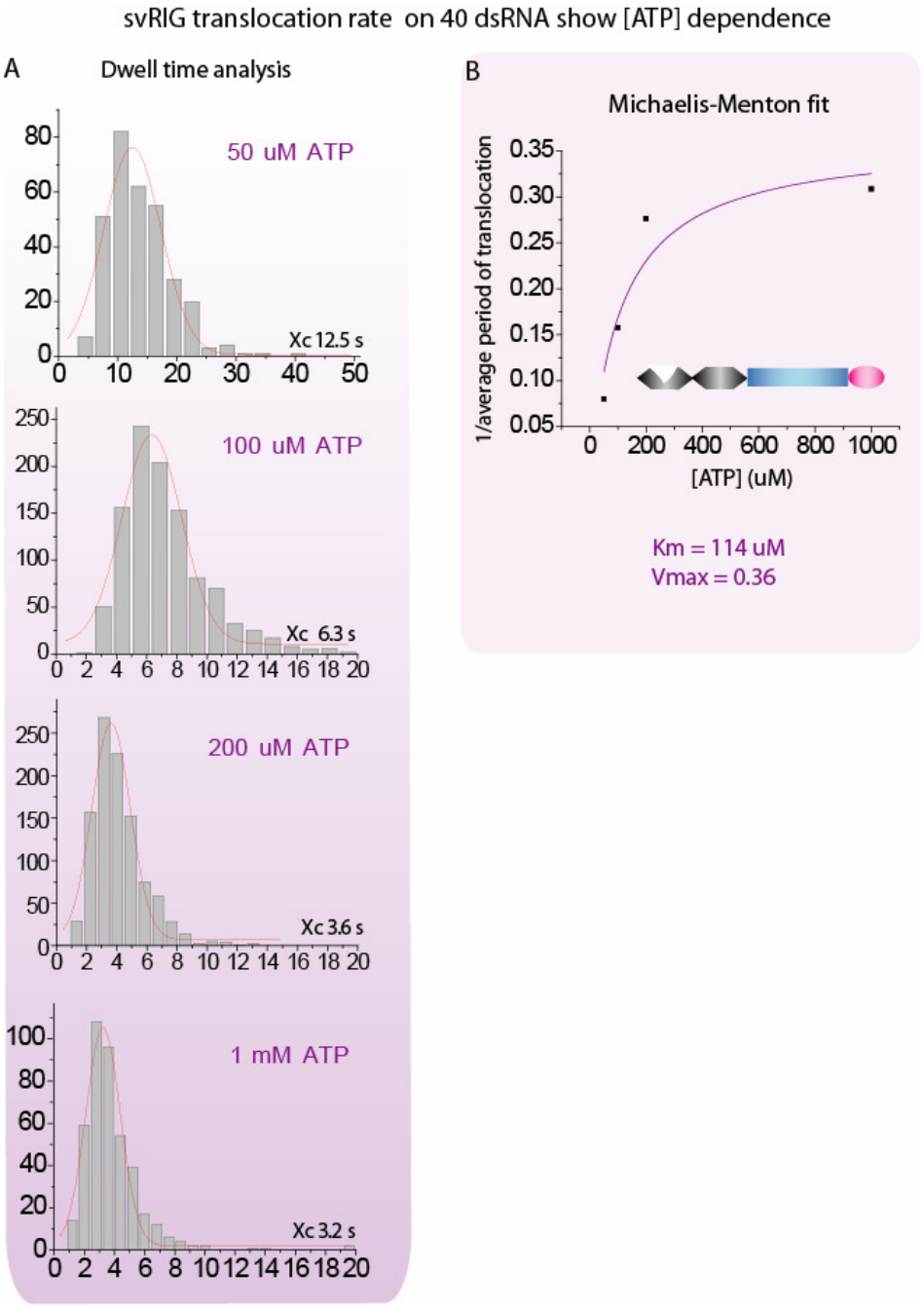

Fig. S5 : RIG-I splice variant translocation is [ATP] dependent. A. Period of translocation performed by RIG-I splice variant was collected from many molecules at different ATP concentrations. The dwell time histograms clearly demonstrate that its translocation is ATP dependent. B. Michaelis-Menten fit yielded K_m of 114 uM, which is very similar to K_m obtained for RIGh (178uM).

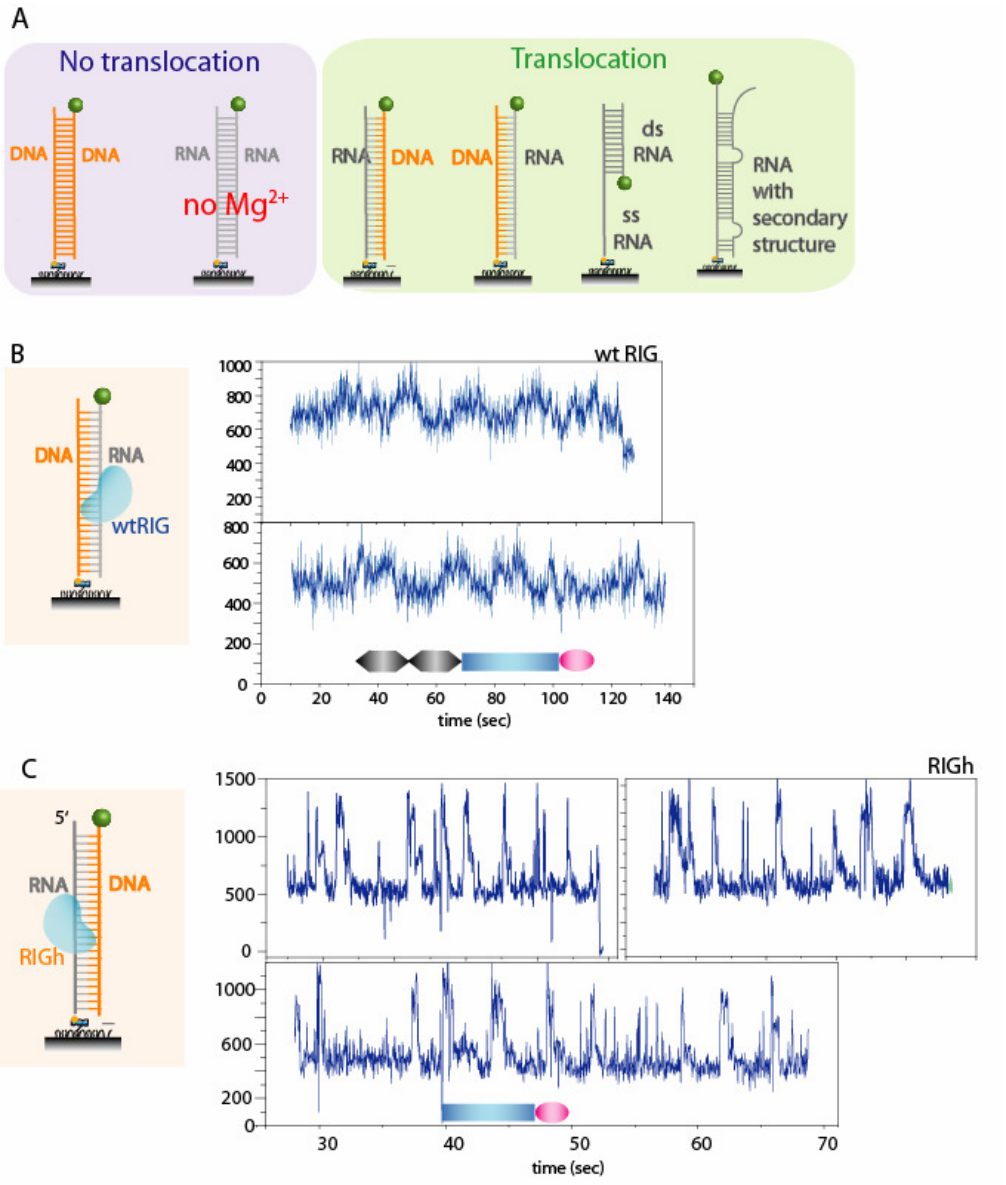

Fig. S6 : RIG-I translocate on RNA:DNA heteroduplex. A. RIG-I shows no translocation on dsDNA or when Magnesium is removed from the buffer. RIG-I showed translocation on RNA:DNA hybrids, partially duplexed RNA or RNA with minor secondary structure. B. DNA:RNA hybrid was made 25bp in length for consistency with the previous measurements. wtRIG showed slow movement, comparable to its activity on dsRNA. C. RIGh showed active translocation on RNA:DNA hybrid, similar to its translocation on dsRNA. This result demonstrates that RIG-I translocation is RNA dependent.

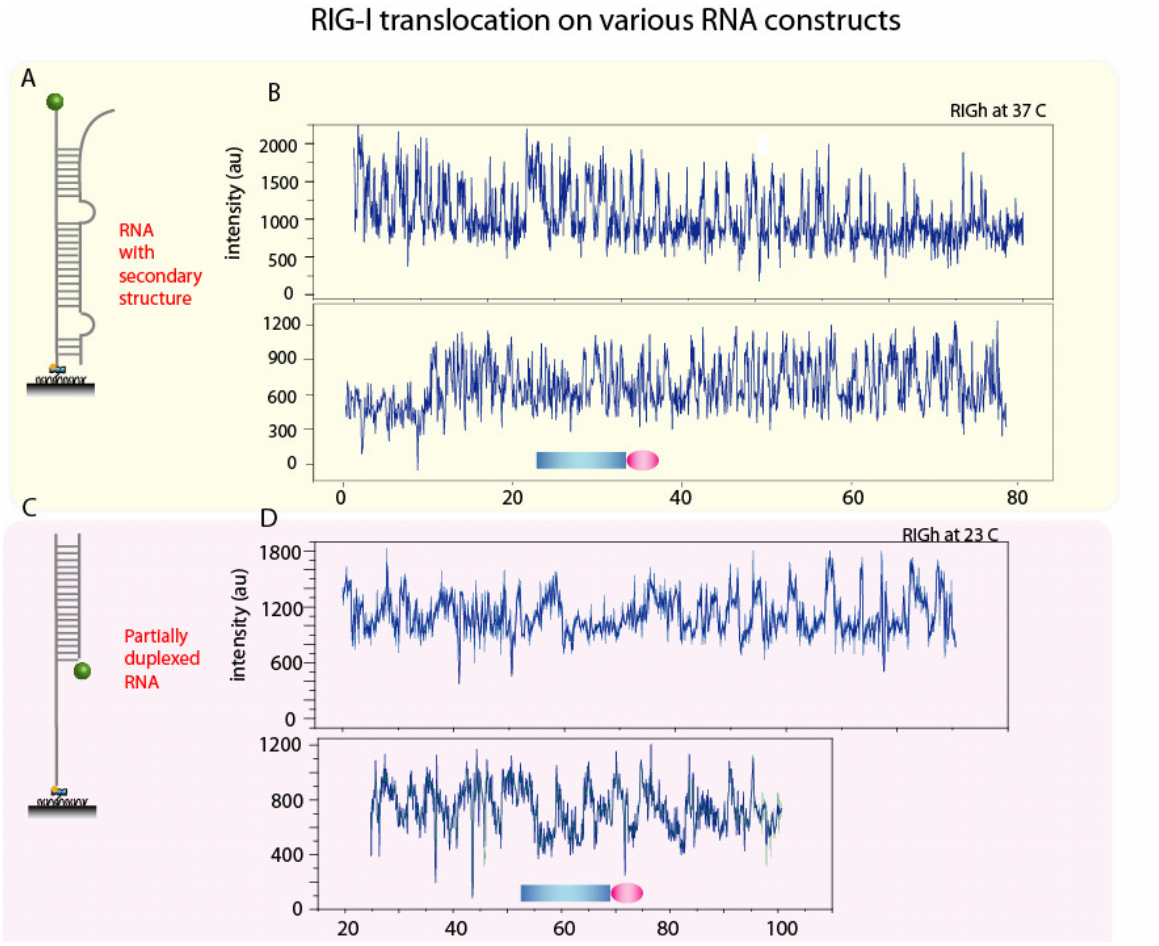

Fig. S7 : RIG-I translocate on various RNA constructs RIG-I showed robust translocation on RNA constructs shown above, and RNA with secondary structure and partially duplexed RNA.

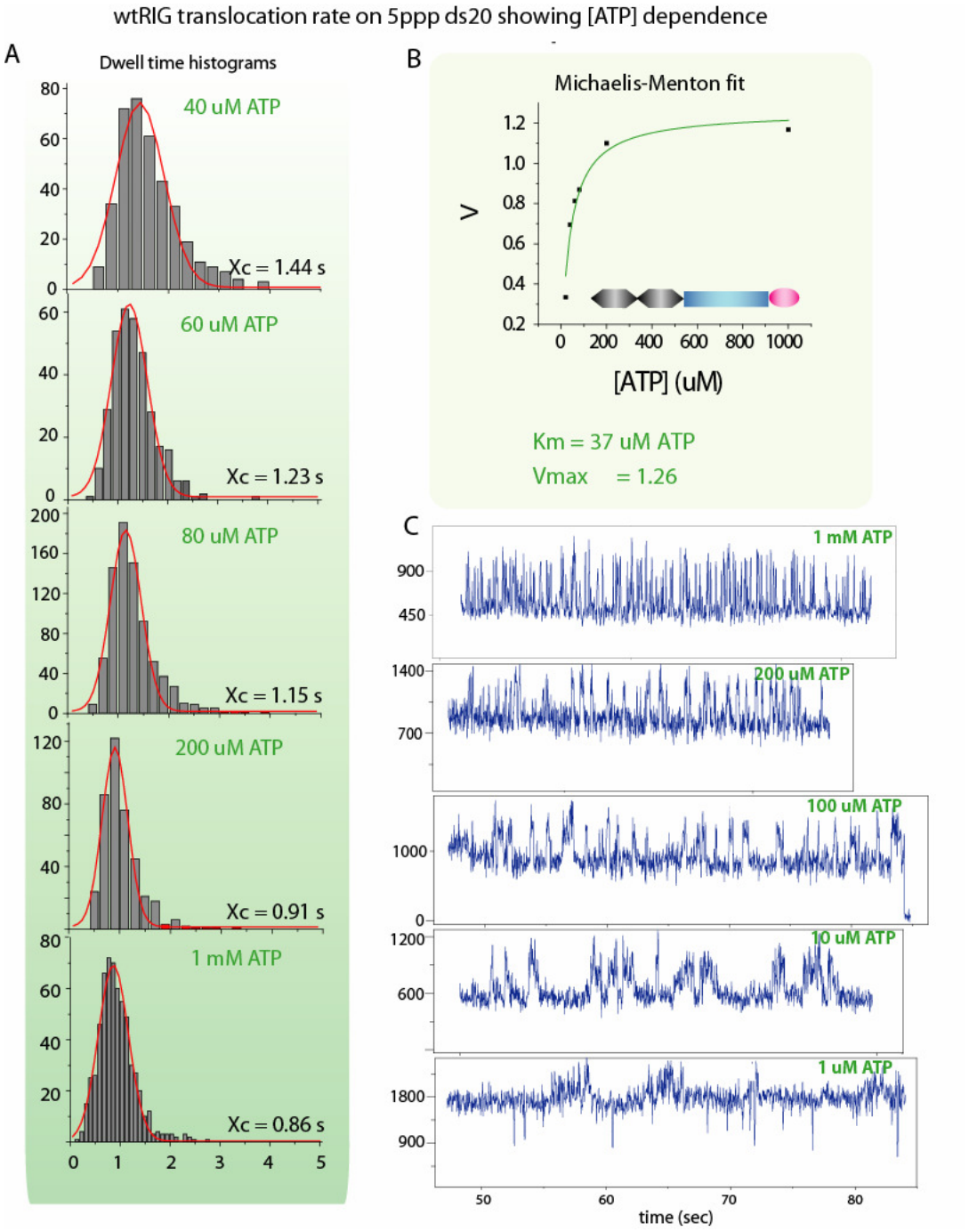

Fig. S8 : wtRIG translocation on 5-triphosphate RNA is [ATP] dependent.
A. wtRIG translocation was measured at different [ATP] and the dwell time analysis was built into histograms. B. Michaelis-Menten fit yielded Km of 37uM ATP, which is much lower than RIGh for the same condition. C. Individual traces also display [ATP] dependent rate of translocation.

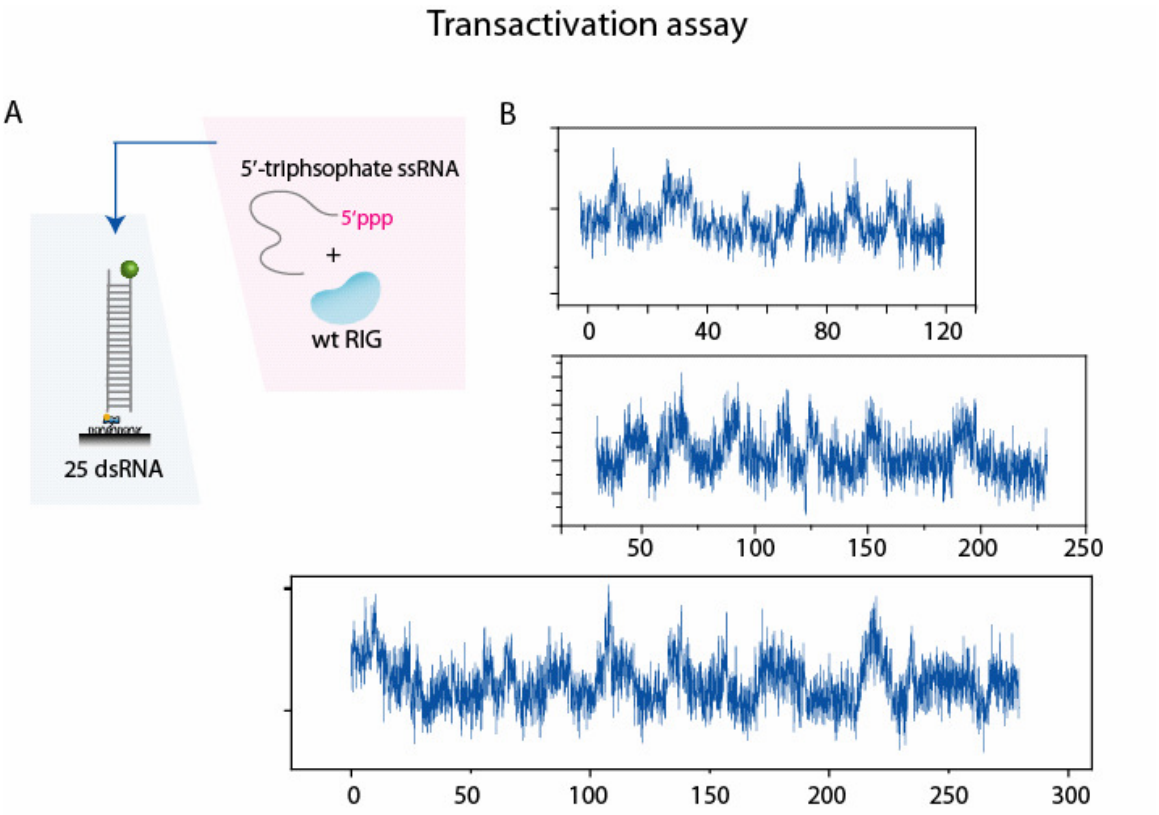

Fig. S9 : *cis* activation of RIG-I A. Transactivation assay was performed to test if external 5'-triphosphate RNA can activate RIG-I and accelerate its translocation on dsRNA. 5'-triphosphate was incubated with wtRIG the added to dsRNA together with ATP. B. As shown, traces reveal that wtRIG movement on dsRNA remained slow and no accelerated movement was observed i.e external 5'-triphosphate RNA was not able to activate RIG-I, confirming *in cis* activation.

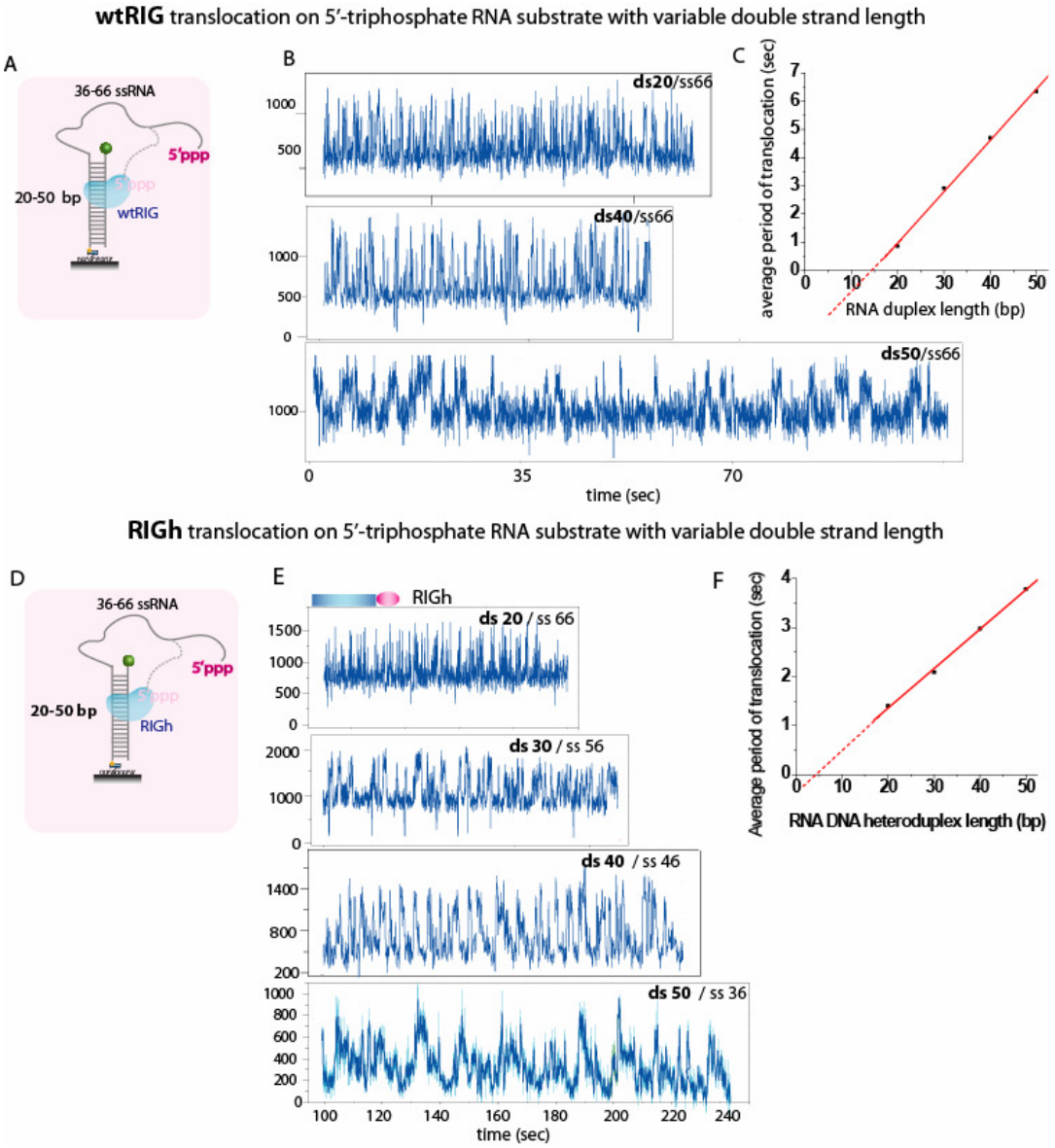

Fig. S10 : wtRIG and RIGh translocate on duplex of 5'-triphosphate pdRNA A, D. The length of duplex was varied from 20 to 50 in 10 bp increment on a partially duplexed RNA with 5'-triphosphate tail. B, E. Traces from 20bp, 40bp and 50bp show duplex length dependent translocation. C, F. The period obtained from the experiment is potted against the length of duplex. It shows that the period is proportional to the length of duplex RNA, not ssRNA.

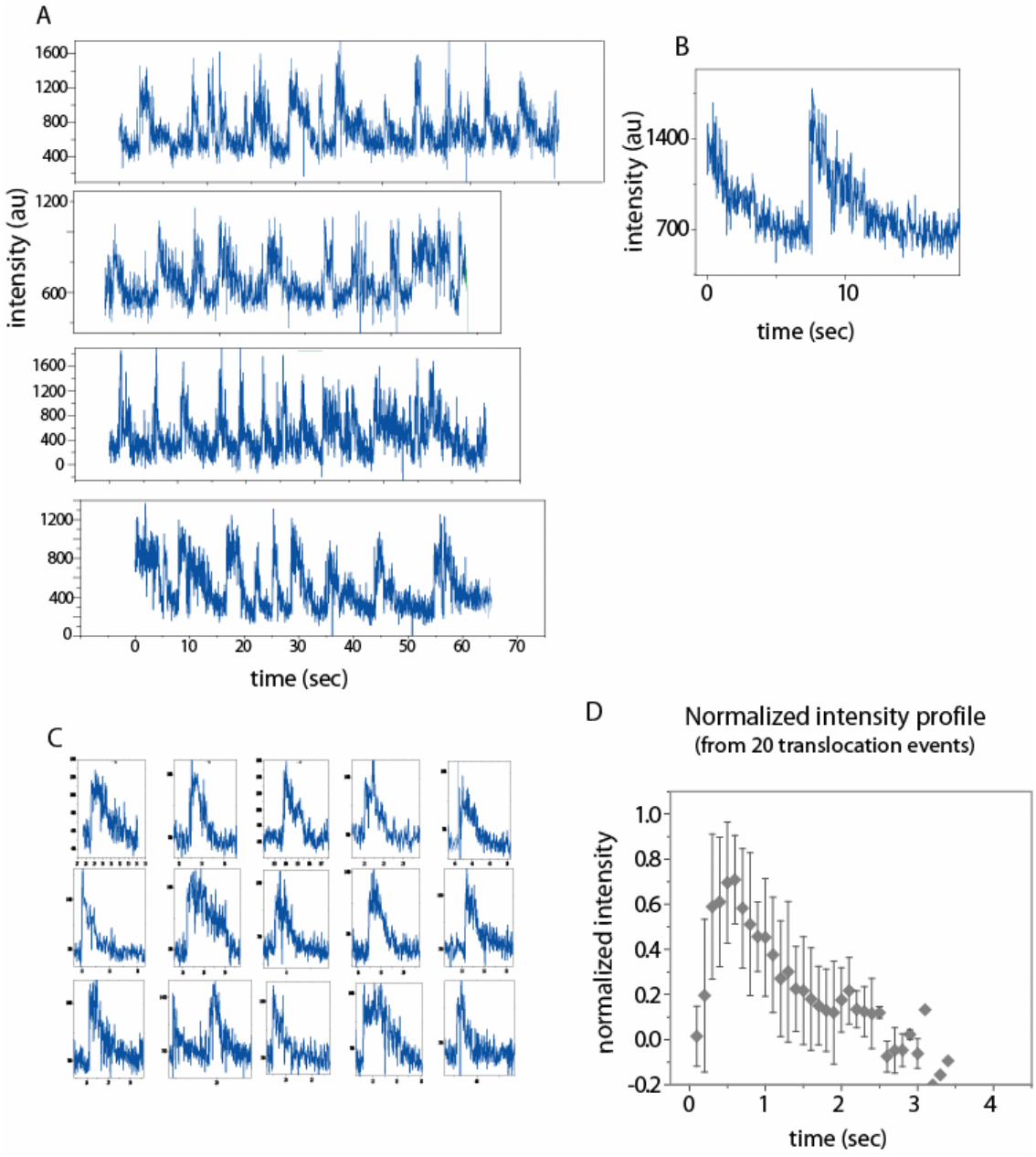

Fig. S11 : Asymmetric translocation displayed by RIGh A. RIGh translocation on 5'-triphosphate 46ss/40ds construct. Data taken at lower ATP (50uM) shows a succession of translocation events exhibiting asymmetric pattern. B. A zoomed-in image also shows an abrupt rise followed by a gradual decrease. C. Twenty events showing asymmetry (1mM ATP) with a similar periodicity were selected and rescaled by normalizing their intensity. The average with error bars are plotted as shown in D.

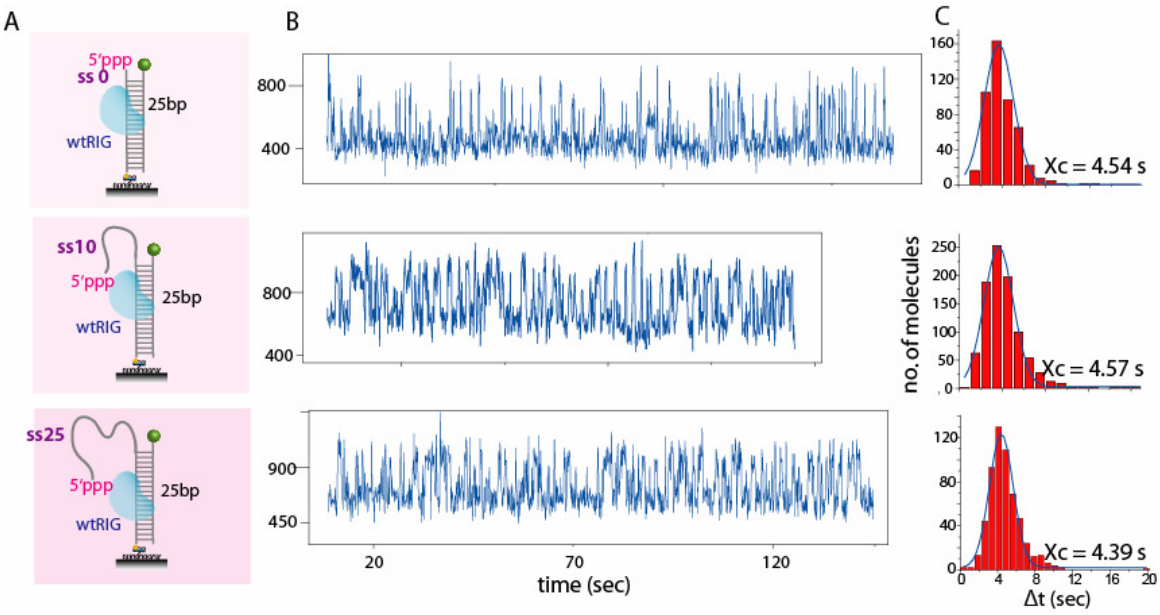

Fig. S12 : RIG-I translocation does not depend on ssRNA tail length. A. dsRNA constructs bearing 5'-triphosphate were prepared to have 0, 10 and 25 ssRNA tail. B. Representative traces from translocation assay of different tail length are shown. C. Dwell time analysis reveals that the rate of translocation was not influenced by ssRNA tail length, confirming that RIG-I translocation is on dsRNA, not on ssRNA.

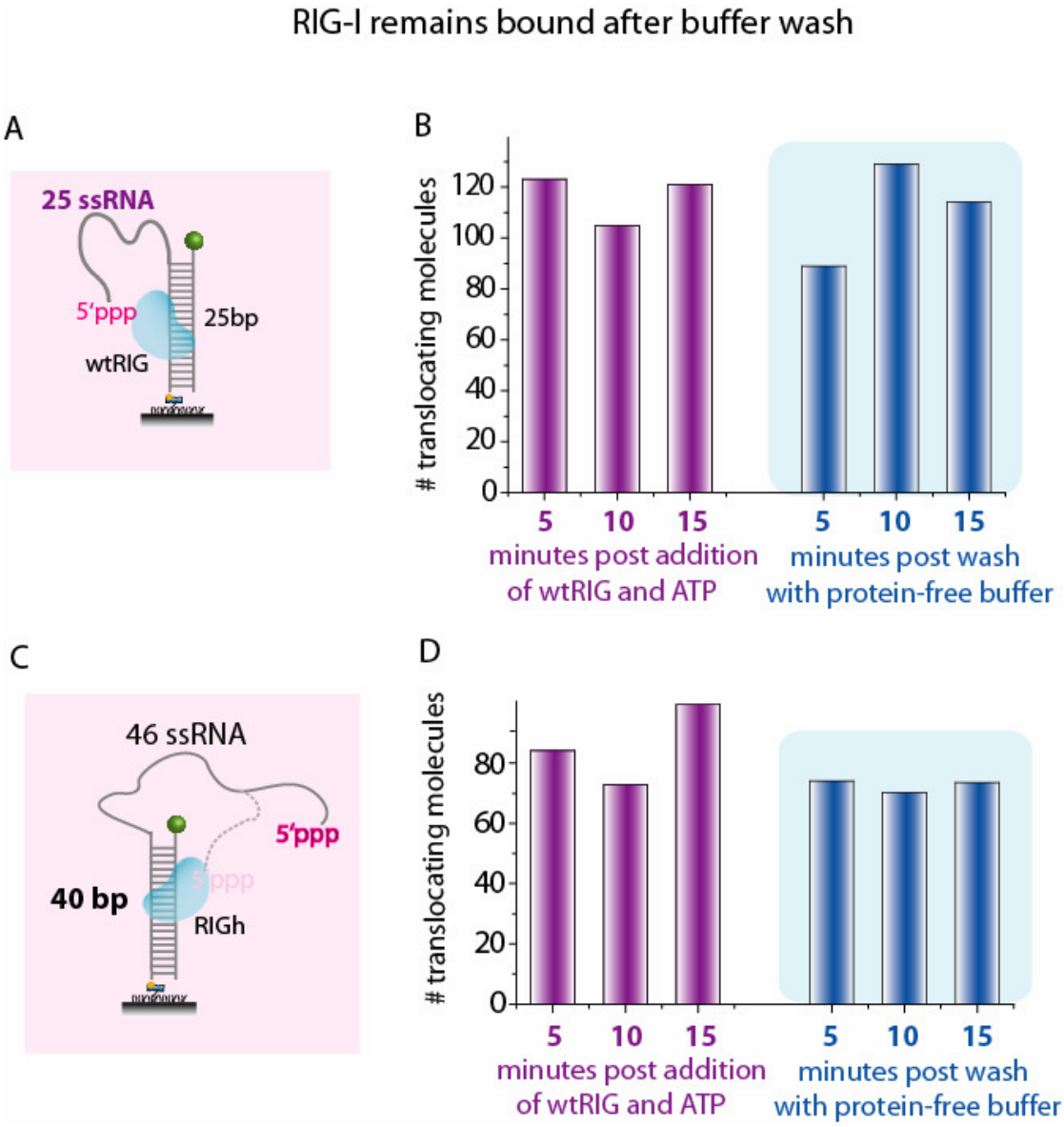

Fig. S13 : RIG-I remains bound after buffer wash A,B Number of translocating molecules were counted from 5 to 15 minutes after the addition of protein (wtRIG)+ATP (purple bars). After the reaction chamber was washed with protein-less buffer containing ATP the number of translocating molecules were counted from 5-15 minutes (blue bars). As shown, majority of molecules remained bound to RNA translocating even after the buffer wash, thus displaying a high processivity on 5'-triphosphate RNA. C,D The same experiment and counting was performed with RIGh and it shows that majority of RIGh remains bound after the protein-free buffer wash.

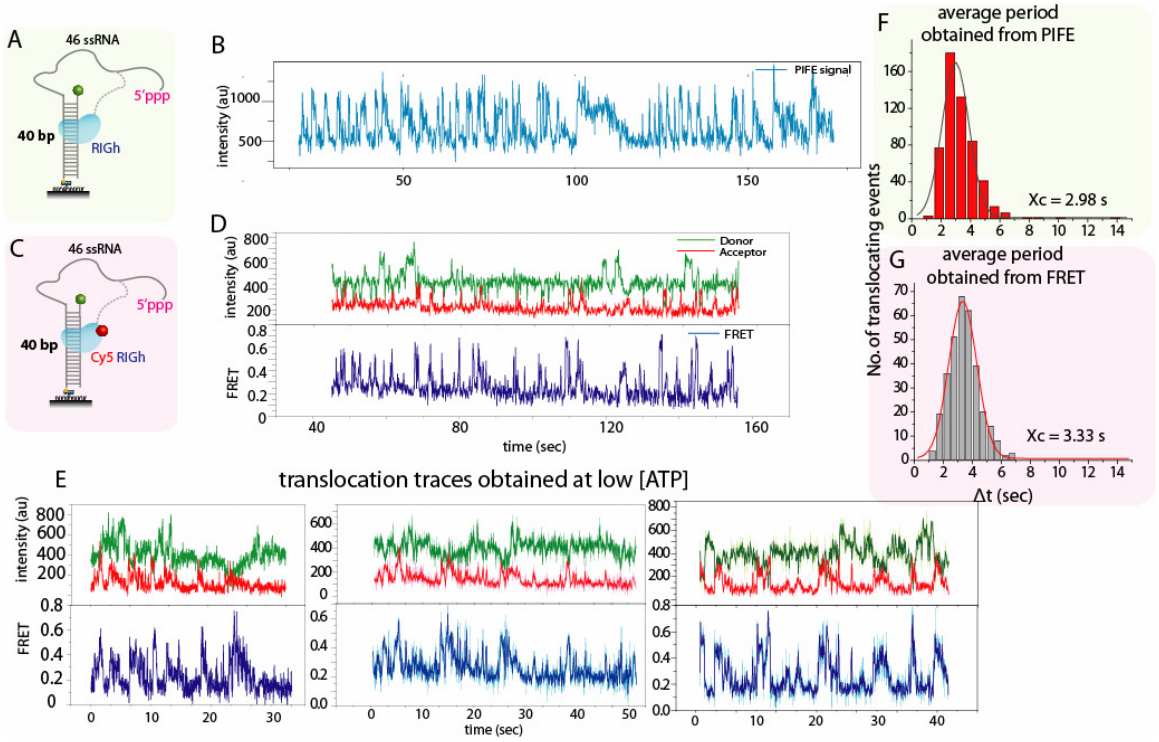

Fig. S14 : Translocation of RIG-I can be visualized by FRET A, B Shown in A and B is the translocation of RIGh on 5'-triphsophate partial duplex monitored by PIFE. The equivalent experiment in FRET is displayed in C-E. RIGh was labeled with Cy5 nonspecifically using maleimide and NHS-ester conjugation and used on the identical substrate as shown in C. C-E. The observed FRET change corresponds to the expected pattern of movement of RIGh on duplex. At lower ATP concentrations, the anti-correlated changes between donor and acceptor can be viewed more clearly (E). F,G Dwell time analysis from PIFE (F) and FRET (G) match closely, further verifying that the signal changes from both measurement report on the same repetitive translocation of RIGh on RNA.

Reference

S1. S. Cui *et al.*, *Mol Cell* **29**, 169 (Feb 1, 2008).
S2. H. Schurer, K. Lang, J. Schuster, M. Morl, *Nucleic Acids Res* **30**, e56 (Jun 15, 2002).
S3. P. Davanloo, A. H. Rosenberg, J. J. Dunn, F. W. Studier, *Proc Natl Acad Sci U S A* **81**, 2035 (Apr, 1984).
S4. T. Ha *et al.*, *Nature* **419**, 638 (Oct 10, 2002).
S5. S. Myong, M. M. Bruno, A. M. Pyle, T. Ha, *Science* **317**, 513 (Jul 27, 2007).
S6. S. Myong, I. Rasnik, C. Joo, T. M. Lohman, T. Ha, *Nature* **437**, 1321 (Oct 27, 2005).